Self Diffusion and Spectral Modifications of a Membrane Protein, the *Rubrivivax gelatinosus* LH2 Complex, Incorporated into a Monoolein Cubic Phase

N. Tsapis,* F. Reiss-Husson,† R. Ober,‡ M. Genest,§ R. S. Hodges,§ and W. Urbach*

*Laboratoire de Physique Statistique de l'Ecole Normale Supérieure, UMR 8550 CNRS, 75231 Paris Cedex 05, †UPR 2167, Centre de Génétique Moléculaire, Bât 24, CNRS, 91198 Gif sur Yvette, ‡Laboratoire de Physique de la Matière Condensée, Collège de France and URA 792 CNRS, 75231 Paris Cedex 05, France, and §Department of Biochemistry, 321A Medical Sciences Building, University of Alberta, Edmonton, Alberta T6G 2H7, Canada

ABSTRACT The light-harvesting complex LH2 from a purple bacterium, *Rubrivivax gelatinosus*, has been incorporated into the Q230 cubic phase of monoolein. We measured the self-diffusion of LH2 in detergent solution and in the cubic phase by fluorescence recovery after photobleaching. We investigated also the absorption and fluorescence properties of this oligomeric membrane protein in the cubic phase, in comparison with its β-octyl glucoside solution. In these experiments, native LH2 and LH2 labeled by a fluorescent marker were used. The results indicate that the inclusion of LH2 into the cubic phase induced modifications in the carotenoid and B800 binding sites. Despite these significant perturbations, the protein seems to keep an oligomeric structure. The relevance of these observations for the possible crystallization of this protein in the cubic phase is discussed.

INTRODUCTION

Incorporation of membrane proteins into lipid bilayers after their isolation in detergent solution is a widespread and powerful approach for the study of their biological activity and structure. Liposomes formed in excess water by a number of phospholipids offer to such a protein an environment milder than a detergent micelle, and which mimics closely its native medium. Furthermore, lipid–water systems provide a rich choice of liquid–crystalline phases, where the short-range disorder of the lipid acyl chains allows for accommodation in the bilayer of the hydrophobic regions of the membrane protein (whether transmembrane α helices or β barrels), while the lipid/water interfaces offer enough space to the hydrophilic parts of the protein. Among these phases, bicontinuous cubic phases, such as those observed in monoglyceride–water systems, are of particular interest. Phase diagrams of monoglycerides are well known; for monoolein/water in particular, two bicontinuous cubic phases, called respectively Q230 and Q224, observed above 20°C, differ in structure and water content (Larsson, 1983; Caffrey, 1987; Qiu and Caffrey, 2000). Both are made up from lipid bilayers, which are continuously folded through the whole space. These bilayers divide the space into two independent subspaces containing water, with the glycerol polar groups located at the lipid/water boundaries. The two phases differ by their symmetry and that of the water channels: Q224 has a primitive cubic unit cell, and Q230 is body centered (Luzzati et al., 1997). During the formation of a monoglyceride cubic phase in presence of a membrane protein in detergent solution, the detergent is presumably diluted into the lipid and the membrane protein is incorporated into the continuous lipid bilayers where it diffuses laterally.

In the pioneering work of Rosenbusch and coworkers (Landau and Rosenbusch, 1996), a membrane protein, bacteriorhodopsin, was incorporated in a monoolein (MO) cubic phase and its crystallization was induced from this phase, yielding crystals of crystallographic quality. This approach seems quite promising (Rummel et al., 1998), and was recently extended to other proteins (Chiu et al., 2000). However, the underlying mechanism of crystallization is still unknown (Caffrey, 2000), and a better characterization of the initial events following the incorporation of the protein would be helpful to shed light on them. This issue is the aim of the present report, where we studied the incorporation of the light-harvesting LH2 complex from a purple bacterium, *Rubrivivax (Rv.) gelatinosus*, into the Q230 cubic phase of monoolein.

This LH2 membrane protein has been isolated in a detergent-solubilized form that retains the in vivo absorbance and the internal energy-transfer properties (Brunisholz et al., 1994; Jirsakova et al., 1996b). Reconstitution in lipid bilayers and two-dimensional crystallization experiments allowed us to determine its oligomeric structure, which is nonameric when associated with lipids (Ranck et al., 2001). It belongs to a structural class that has been described at the atomic level for two purple bacteria (MacDermott et al., 1995; Koepke et al., 1996), and at a lower resolution for two other species (Savage et al., 1996; Walz and Ghosh, 1997). These complexes are oligomers of a basic unit composed of a heterodimer of two short polypeptides (α and β), each containing a single transmembrane α helix. The pigments, composed of three bacteriochlorophylls (Bchl) and one carotenoid per heterodimer, are buried within the helices.

Received for publication 25 May 2000 and in final form 19 May 2001.

Address reprint requests to Francoise Reiss-Husson, UPR 2167, Centre de Génétique Moléculaire, Bât 24, CNRS, 91198 Gif sur Yvette, France. Tel.: 33-1-69-82-3830; Fax: 33-1-69-82-3802; E-mail: freiss@cgm.cnrs-gif.fr.

0006-3495/01/09/1613/11 $2.00

Several of these basic units (either 8 [Koepke et al., 1996] or 9 [MacDermott et al., 1995; Savage et al., 1996; Walz and Ghosh, 1997]) are associated to form a hollow cylinder, with the cylinder axis roughly parallel to the transmembrane α helices. The outer surface of the cylinder is formed by the β subunits, and its inner surface by the α ones.

The LH2 is representative of membrane proteins that are strongly hydrophobic and devoid of large hydrophilic parts. In the present work, its incorporation into the MO Q230 cubic phase was studied by small x-ray scattering. The lateral diffusion coefficient of the protein was determined in this phase by following the fluorescence recovery after photobleaching, and its value was compared to that measured in the detergent-solubilized state. The small-angle x-ray scattering experiments indicated that low amounts of LH2 do not perturb the cubic-phase structure, where the complex probably exists in an oligomeric state. A phase transition to the lamellar L_α phase was, however, triggered when the concentration of protein was higher. Absorbance and steady-state fluorescence measurements indicated that some pigment–protein interactions and the inter-pigment energy transfer were modified in these MO liquid–crystalline phases. These changes were restricted to the carotenoid and to the most solvent-exposed Bchl molecules, revealing a partial opening of these pigment-binding sites.

EXPERIMENTAL PROCEDURES

Materials

Monoolein (1-monooleoyl-rac-glycerol, M = 356.5, denoted MO) was obtained from Sigma (St. Quentin, France) (purity ~99% as indicated by the provider) and used without further purification. Monoolein density has been taken equal to 1g/ml. Octyl-β-D-glucopyranoside (OG, M = 292.4, cmc $\approx$ 26 mM, e.g., 7.8 mg/ml (Kameyama and Takagi, 1990)) was purchased from Bachem (Basel, Switzerland), and lauryl-dimethylamineoxide (LDAO) from Fluka (St. Quentin, France). 1,3-bis-[tris(Hydroxymethyl)-methylamino]-propane (BisTris-propane, M = 282.3) was purchased from Sigma-Aldrich. (*N*-octadecanoylamino)fluorescein (C_{18}FLUO, M = 613) was purchased from Molecular Probes (Eugene, OR), and 5-Carboxyfluorescein *N*-hydroxysuccinimide ester (FLUOS) from Boehringer (Mannheim, Germany). All other chemicals were of reagent grade. Water was purified using a Milli-Q system from Millipore (St. Quentin, France). The 250-μl gas-tight syringes used to build the mixing device described below were purchased from Hamilton (Bonaduz, Switzerland) (1725 RN, part 81165) as well as the additional nuts (No. 30902) and needles (No. 22-51-3, 0.41-mm internal diameter).

LH2 isolation and fluorescent labeling

The LH2 complex was isolated from photosynthetically grown *Rv. gelatinosus* cells after solubilization of the membranes with LDAO, followed by chromatographic purification according to a published protocol (Jirsakova et al., 1996b) with slight modifications (Ranck et al., 2001). In the purified preparation, LDAO was finally exchanged for 27 mM (8 mg/ml) OG by adsorption of the protein on a small di-ethyl aminoethyl-Sepharose Fast Flow (Pharmacia, Uppsala, Sweden) column: the gel was washed extensively with a 10-mM BisTris-propane buffer, pH 9.0, containing 8 mg/ml OG and 1 mM EDTA, then the protein was eluted with 0.2 M NaCl in this buffer. Alternatively, LDAO was exchanged for 27 mM OG by repetitive cycles of concentration, followed by dilution with OG-containing buffer, using Amicon XM-50 (Millipore) ultrafiltration membranes. Exchange of buffer when needed was performed either by dialysis or on a Sephadex PD10 (Pharmacia) gel filtration column.

Fluorescent labeling of the isolated LH2 (2 mg/ml) was performed by incubation at 22°C with 3 mM FLUOS (added from a 0.3 M stock solution in dimethylsulfoxide, 20-fold molar excess of reagent over protein) in a 50 mM HEPES buffer (Sigma), pH 7.5, containing 1 mg/ml LDAO. The preparation was put on ice and most of the excess FLUOS was eliminated by chromatography first on a Sephadex PD10 column equilibrated in the same buffer, then on a Biogel P6DG (Biorad, St. Quentin, France) column. On both columns, most of free FLUOS was retarded and separated from the protein that was recovered in the void volume but still contained some residual free FLUOS. Exchange of LDAO for OG was then performed as described above by several cycles of concentration by ultrafiltration on Centricon 100 units (Millipore) followed by dilution with 27 mM OG-containing buffer. This allowed, at the same time, separation of the protein from the last amounts of free FLUOS, which were eliminated in the successive ultrafiltrates, as judged from their visible absorption spectrum.

Purity of the various preparations was evaluated by SDS-PAGE on 16.5% acrylamide minigels (0.75-mm thickness) (Schägger and Von-Jagow, 1987), which were stained with Coomassie Brilliant Blue G250. For FLUOS-labeled preparations, illumination of the gels with UV light before staining was used to determine if one or both LH2 polypeptides were labeled. The extent of FLUOS labeling was determined in a difference spectrum by the increased absorbance at 498 nm (as compared with the unlabeled sample) using for FLUOS an extinction coefficient $\epsilon_{mM} = 74$ (as indicated by the manufacturer).

The protein concentration was determined by its absorbance, using for the $Bchl_3(\alpha\beta)$ protomer an extinction coefficient $\epsilon_{mM} = 382$ at 854 nm (Jirsakova, 1995). Because the molecular weight of $(\alpha\beta)$ is 12,531, according to the gene sequence (accession number: AF312921), 1 mg/ml protein corresponds to A = 30.5 at 854 nm.

Fluorescent peptide

The sequence of the transmembrane fluorescent peptide is the following: Lys-Lys-Gly-$(Leu)_{12}$-Lys-Lys-Ala-amide and the N-terminus is derivatized with a fluoroscein-isothiocyanate (FITC) group. The FITC has a mass of 389 Da. The whole peptide has a mass of 2405 Da. It was synthesized using standard Tert-butyloxycarbonyl group (Boc) chemistry as described (Sereda et al., 1993) except for the following differences: the side chain on Lys was the 9-fluorenylmethoxycarbonyl (Fmoc); the peptide was cleaved using no anisole or ethanedithiol; and the Boc group was removed before cleavage and the N-terminal was left free. The crude peptide was then dissolved in dimethylformamide:dichloromethane:hexafluoroisopropanol 80:15:5 (v:v:v) and then reacted with two equivalents each of 1-3-diisopropylethylamine and FITC for 4 hrs. Excess FITC was then removed using 20% piperidine for 1 hr. The solution was rotoevaporated and purified to 95% by reversed-phase high pressure chromatography (Sereda et al., 1993) on a Phenomenex Luna (Torrence, CA) (250 mm x 21 mm) column, using a linear gradient of 2% B/min starting with 100% A, where A = water and B = isopropanol.

Preparation of the cubic phase samples

Cubic phases of MO containing 30–33% water (w/w) were prepared according to two different methods. The first one consists in mixing MO with aqueous buffer (eventually containing detergent and protein) by centrifugation (3 hrs, 10,000 $\times$ *g* at 22°C) in an Eppendorf desktop centrifuge. This method is the most common and has been extensively used (Rummel et al., 1998). The other one uses a mixing device (Cheng et al., 1998) that we simplified slightly. Briefly, two 250-μl gas-tight microsyringes are joined by a small-bore coupling needle, through two nuts

soldered together. Dry MO is weighed in one syringe, and buffer solution is weighed in the other one. They are then linked, and mixing is achieved at 22°C by cycling approximately 100 times the mixture from a syringe to the other through the needle. Homogenization of the mixture can be checked through the transparent syringe body. The cubic phase is then transferred for experiments. This second method allows preparation of samples more rapidly and avoids prolonged incubation at 22°C, which can damage some proteins. Optical isotropy of all samples has been checked between crossed polarizers. The fluorescein-labeled amphiphile C_{18}FLUO was weighed in aqueous buffer in low concentration (5×10^{-3} M) and then mixed with dry MO using the methods described above.

For preparing a LH2-containing cubic phase, 50 mg MO were mixed with 23 μl of an LH2 solution at an appropriate protein dilution in a 50-mM BisTris-propane buffer, pH 9.0, containing 0.1 M NaCl and 27 mM OG. The final concentrations were 8.5 mM OG (2.5 mg/ml) and 68% MO, which corresponded to a weight ratio of OG-to-MO of 1:270. The concentration of protein was 0.4 mg/ml for the spectroscopic measurements, and 4.8 mg/ml for some x-ray experiments (weight ratio of protein-to-MO respectively, 1:1700 and 1:140).

The peptide-containing cubic phase was prepared by adding 0.5 mg lyophilized peptide to 40 mg MO powder. The rest of the preparation is similar to what is presented above.

Preparation of the lamellar phase samples

Lamellar (L_α) phases of MO containing 15% aqueous buffer (w/w) were prepared by adding to 90 mg MO 15 μl of a 50-mM BisTris-propane buffer, pH 9.0, containing 0.1 M NaCl and 27 mM OG, and centrifuging 1 hr, at 10,000 $\times$ g and 22°C in an Eppendorf desktop centrifuge. Then, 1 μl of protein-containing buffer was added; the sample was vortexed and let to equilibrate at 25°C until a homogeneous coloration was observed. We verified at that stage that the textures observed with a polarizing microscope were typical of a smectic phase. The aqueous compartment represented 15% of the sample. The final concentrations were 0.1–0.2 mg protein/ml and 4 mM OG.

Preparation of a LH2 sample in a MO/OG aqueous dispersion

In an Eppendorf tube, 491 mg of 50-mM BisTris-propane buffer, pH 9.0, containing 0.1 M NaCl and 27 mM OG were added at 20°C to 15 mg MO. The sample was centrifuged 30 min at 13,000 $\times$ g and sonicated for 10 min in a water bath (Branson B200, Sigma). One hundred microliters of an LH2 solution in the same buffer were added at 20°C with stirring. The MO content was 2.47%. The final concentration of protein was 0.055 mg/ml and that of OG was 26 mM.

Spectroscopic methods

Absorption spectra were obtained with a Cary 2300 (Varian, Palo Alto, CA) recording spectrophotometer interfaced with a computer and analyzed using Origin (Microcal) software. Steady fluorescence spectra were recorded on a Perkin-Elmer (Courtaboeuf, France) LS50B luminescence spectrometer. For these measurements, cubic and lamellar phase samples were pressed between the quartz windows of a two-part cuvette (Hellma type 106, 0.2 mm optical path, Mühllheim, Germany). Sample temperatures (22°C for the cubic phase and 25°C for the lamellar phase) were maintained by a thermostated bath with an accuracy of $\pm$0.1°C.

The fringe pattern fluorescence after photobleaching technique

The fluorescence recovery after photobleaching (FRAP) technique, used to measure self-diffusion of fluorescent probes in mesophases of surfactants and lipids, has been described in detail elsewhere (Messager et al., 1988). Briefly, a very short powerful laser pulse induces irreversible destruction of the fluorescent groups in a sample where a fluorescent probe has been homogeneously dissolved. The fluorescence signal is then monitored using a less powerful laser beam as diffusion of the probes leads to a new homogeneous concentration in the region of the sample where fluorescence has been destroyed. The bleaching pulse has been achieved with a Spectra Physics (Les Ulis, France) argon laser (500 mW at 488 nm); the weaker beam has a 1000$\times$ smaller power at the same wavelength. The bleaching and the monitoring beams are both divided and superposed in the sample to create a fringe geometry. After the bleaching pulse, to reduce the signal-to-noise ratio in the recovery exponential signal, a piezo-electric crystal makes the monitoring beam sweep the bleached fringes in the sample. The sample intensity was measured either by a photomultiplier for measurements in the visible range, or by an avalanche photodiode (C5460–01, Hamamatsu, Hamamatsu City, Japan) for measurements in the infrared range. Using the classical relation $D = i^2/4\pi^2\tau$, where the interfringe values i are in the 10–100-mm range, and τ is the characteristic recovery time, one can deduce the diffusion coefficient. The self-diffusion coefficients obtained with this method exhibit an error smaller than 5%. Samples were put in Hellma quartz cells of 1-mm path length, and maintained at 22°C by a thermostated bath with an accuracy of $\pm$0.1°C.

Small angle x-ray scattering experiments

Small angle x-ray scattering experiments were performed at 22°C with a rotating anode (Rigaku, Japan) with a copper target (λ = 1.54 Å) and an effective source size of 0.1 $\times$ 0.1 mm^2. Samples were put between two mica sheets separated by 1 mm thick Teflon™ wedges, and placed in a sample holder whose temperature was regulated by a thermostated bath (Haake C25) with an accuracy of $\pm$ 0.1°C. The distance between the linear detector (512 channels) and the sample holder was 37 cm. The scattered intensity was corrected from the absorption of the sample. The background scattering of pure solvent and mica was measured and subtracted from the sample signal. The wave vector q is defined as follows: $q = 4\pi\sin(\theta/2)/\lambda$ where λ is the wavelength (1.54 Å), and θ the angle between the direct and scattered beams. The Bragg distance is then defined as $d_B = 2\pi/q$. Spectra have been accumulated for 3 h for each sample.

RESULTS AND DISCUSSION

Fluorescent labeling of the LH2 protein

In the known LH2 structures, the Bchl molecules are distributed in two pools that differ in structure and spectroscopic properties (Freer et al., 1996). One pool that absorbs in the infrared range at or near 850 nm forms a continuous ring of strongly coupled molecules (called B850) sandwiched between the α and β hydrophobic helices. The other Bchls (B800, absorbing at ~800 nm) are located nearer the cytoplasmic side of the protein and form a second ring between the β hydrophobic helices; their excitonic interactions are weaker than those of the B850. The extended carotenoid molecule of each motive spans the whole hydrophobic region from the cytoplasmic side to the periplasmic one. Within this assembly, light energy is transferred from the short-wavelength-absorbing pigments (carotenoids, and the B800-Bchls) to the longest-wavelength-absorbing ones (B850-Bchls). In the isolated LH2, most of the light excitation is finally reemitted as fluorescence from B850, whereas, in the membrane, it is transferred from B850 to

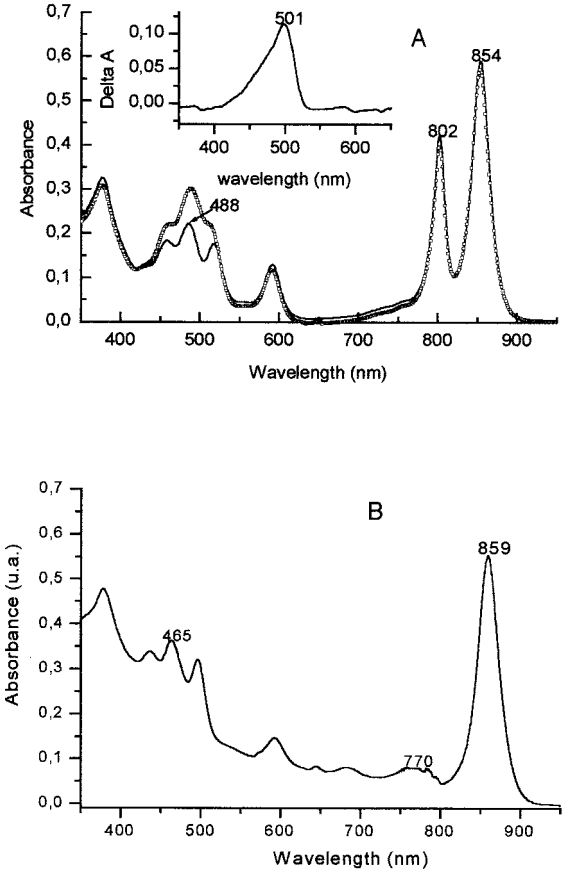

FIGURE 1 Absorption spectra of LH2 samples under various conditions. (*A*) Samples in detergent solution: comparison of LH2 (*solid trace*) and FLUOS-LH2 (*squares*), both in a 50-mM BisTris-propane buffer, pH 8.5, containing 8 mg/ml OG. Spectra have been normalized to the same IR absorbance. *Inset:* difference spectrum showing the contribution of the FLUOS label to absorbance. (*B*) LH2 sample after incorporation in the MO Q230 cubic phase.

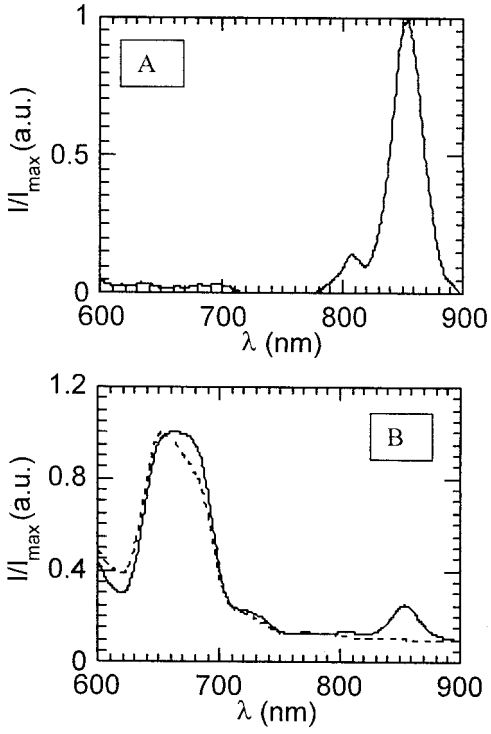

FIGURE 2 Fluorescence emission spectra of various LH2 samples excited at 488 nm. (*A*) LH2 sample in OG solution, same conditions as in Fig. 1 *A*. (*B*) Emission spectra of LH2 in the presence of a dispersion of MO in excess water (*solid trace*) and of LH2 incorporated in the MO Q230 cubic phase (*dotted trace*). Spectra have been arbitrarily normalized to the same emission at 660 nm.

another light-harvesting complex and finally to the reaction center.

The absorption spectrum of *Rv. gelatinosus* LH2 in OG solution is presented in Fig. 1 *A*. The visible bands peaking at 460, 487, and 518 nm are attributed to the carotenoids, the 590-nm band to the Q_x transition of the Bchls, and the bands located at 800 and 854 nm to the Q_y transitions of the B800 and B850 Bchls, respectively. In the experimental set-up used for the FRAP experiments, the fluorescence was excited at 488 nm, that is, in the visible absorption bands of the LH2-bound carotenoids. These accessory pigments are known to transfer the light energy to the Bchl molecules, leading to the emission at 850 nm from the dimeric B850 Bchls (Fig. 2 *A*). The infrared fluorescence of LH2 in vitro is, however, weak and difficult to detect. We therefore coupled the protein to a strongly fluorescent label that could be excited at 488 nm. The reagent used is the FLUOS (maximum absorption at 494 nm, emission at 518 nm) of the fluorescein family, which is able to react with primary amine groups to form stable amide bonds.

Absorption spectra of native and FLUOS-labeled LH2 (Fig. 1 *A*) were identical in the infrared range, indicating that the label did not perturb the Bchls binding sites. In the visible region, the labeled FLUOS-LH2 showed an increased absorbance peaking at 490 nm, superimposed on the carotenoid absorption bands; this presumably originated from the bound FLUOS. Difference spectra (FLUOS-LH2 minus native LH2) (Fig. 1 *A*, *inset*) showed an absorption band peaking at 501 nm, with a intensity indicating the presence of 0.95 mol of FLUOS/mol of $\alpha\beta$ subunit. In contrast, the examination of unstained SDS-PAGE gels under UV light disclosed two fluorescent bands that migrated at the position of the α and β polypeptides. These observations suggest that the labeling occurred at random on only one polypeptide of the ($\alpha\beta$) pair. Because the reagent is water soluble, it should react with residues accessible on the hydrophilic surfaces of the complex, such as the N-termini or exposed lysines (α Lys 5 or β Lys 7). Excitation of FLUOS-LH2 at 488 nm in detergent solution showed a strong emission at 518 nm as expected (not shown).

TABLE 1 Structural parameters at 22°C of an MO Q230 cubic phase containing or not the LH2 protein at low concentration, prepared as described in Methods

Indices (hkl)	d_B (Å)	a (Å)
211	53.5 ± 1	131 ± 2
220	46.0 ± 1	130 ± 2
321	35.0 ± 0.5	131 ± 1
400	32.3 ± 0.2	129 ± 1
420	28.9 ± 0.3	129 ± 1
332	27.7 ± 0.3	130 ± 1

The diffraction lines corresponding to Bragg spacings d_B are indexed according to a body-centered cubic lattice of parameter a.

The structure of the Q230 cubic phase is not modified by the incorporation of the LH2 protein in small concentrations

Small-angle x-ray scattering was used to check possible modification of the Q230 cubic phase under our experimental conditions. In these experiments, the aqueous component of the samples was kept at 32% (w/w) and the temperature was 22°C. The x-ray spectrum did not change whether this cubic phase was prepared with water or with the aqueous BisTris-propane buffer (without OG).

Because the protein was solubilized in 27 mM OG, we checked the effects of various OG concentrations. Spectra did not vary from 0 up to 54 mM OG in this buffer (not shown). This corresponded to final OG concentrations up to 20 mM, (weight ratio of OG-to-MO 1:100). As already observed (Landau et al., 1997), MO cubic phases are structurally stable: additives such as salts, or some surfactants at low concentration, do not induce any changes in the cubic structure. However, a transition to a lamellar phase can occur (Ai and Caffrey, 2000) but at much higher levels of surfactant than those used here. We also checked that the presence of 5 mM C_{18}FLUO, which is a probe incorporated in the bilayer (Maldonado et al., 1997), did not modify the MO Q230 cubic phase. The presence of the peptide was also without effect on the x-ray diagram.

Finally, the inclusion of LH2 at the low concentrations required for spectroscopic measurements did not modify the structure of the Q230 cubic phase nor the lattice dimensions, whether the protein was FLUOS-labeled or not. As a matter of fact, the final concentrations of protein (0.4 mg protein/ml, weight ratio of protein-to-MO 1:1700) and of OG (8.5 mM) used in these experiments were low enough to not perturb the system. In all these cases, six Bragg peaks could be distinguished (Table 1) at wave vectors q_i. The ratios q_i/q_1 are, respectively, 1.162, 1.538, 1.658, 1.854, and 1.94 for $i = 2–6$ and correspond to $(4/3)^{1/2}$, $(7/3)^{1/2}$, $(8/3)^{1/2}$, $(10/3)^{1/2}$, and $(11/3)^{1/2}$. These ratios are typical of a body-centered cubic lattice (Guinier, 1952); the reflections could be indexed to the following (hkl) indices: (211), (220), (321), (400), (420), and (332). In Table 1, the different Bragg distances and the corresponding lattice parameters are presented, leading to a lattice parameter $a = 131 \pm 3$ Å. This value is in very good agreement with parameters measured by Larsson (1983) and slightly smaller than in Briggs et al. (1996).

However, when the protein concentration was increased 10-fold (final concentration 4.8 mg/ml) while keeping the same volume of aqueous phase added to MO as above, the x-ray diagram changed. Four Bragg peaks could be distinguished at wave vectors q_i: 0.1102, 0.1347, 0.2125, and 0.269 $Å^{-1}$. The ratio $q_3/q_1 = 1.928$ is close to $(11/3)^{1/2}$, which corresponds to the 211 and 332 peaks of a Q230 cubic phase. The corresponding lattice parameter is equal to 139 ± 0.1 Å. The ratio $q_4/q_2 = 1.997$: these peaks can be the first and second order of a coexisting lamellar phase of period $d_B = 46.5 \pm 0.5$ Å. In such a sample, the final amount of OG brought by the buffer was still the same (corresponding to 8.5 mM), and presumably could not be at the origin of the phase diagram change, as indicated by the control experiments performed with OG in the absence of protein (see above). The phase transition was probably induced by the higher protein-to-MO molar ratio. This result is in agreement with the observations of W. Rowe (University of Manchester Institute of Science and Technology, Manchester, U.K., personal communication), who studied the effect of bacteriorhodopsin concentration on the structure of the MO cubic phase.

Self diffusion coefficient of LH2 in the micellar OG solution and in the MO cubic phase as measured by FRAP

The LH2 complex is stabilized in OG micelles as proved by its absorption spectrum (Fig. 1 *A*). To estimate the size of the OG-LH2 complex, FRAP experiments were performed on the protein in presence of 8 mg/ml OG in BisTris propane buffer. Only protein-containing micelles are detectable with this technique (nonfluorescent micelles, e.g., without LH2, are invisible). For small volume fractions ϕ of diffusing objects, the measured self-diffusion coefficient D_{eff} can be written as a development in ϕ:

$$D_{eff} = D_0 (1 + \alpha\phi + \cdots),$$

where α depends on interactions between diffusing objects (here protein–detergent complexes). For hard spheres, according to theoretical predictions, the value of α is between -2.5 and -1 (Evans and James, 1983). The hydrodynamic radius R can be deduced from D_0 using the Stokes–Einstein formula,

$$D_0 = k_B T/6\pi\eta R,$$

where k_B is the Boltzman constant and η the viscosity of the solvent. One can obtain D_0 by diluting the solutions and extrapolating to zero volume fraction of the complexes. In the present case, because the volume fraction of the com-

TABLE 2 Values of self-diffusion coefficients measured at 22°C in various samples and comparison with published values

Phase	Sample	D_0 ($cm^2 s^{-1}$)	Reference
Detergent solution	LH2/OG	$7 \pm 0.4\ 10^{-7}$	This work
	LH2/LDAO	$2.5\ 10^{-7}$	Jirsakova et al., 1996a
Q230 cubic phase	C_{18}FLUO*	$6.2 \pm 0.2\ 10^{-8}$	This work
	$C_{18}{}^{12}$MS†	$6.0 \pm 0.5\ 10^{-8}$	Cribier et al., 1993
	FITC-Peptide	$2.4 \pm 0.2\ 10^{-8}$	This work
	LH2-FLUOS	$1.4 \pm 0.2\ 10^{-8}$	This work

*Lipid probe, see Methods.
†Lipid probe, 1-[12-(7-nitrobenz-2oxa-1,3-diazole)]-monostearin.

plex is $\sim 10^{-3}$, one can consider that the complexes are very far from each other and that their interactions can be neglected. Thus, the diffusion coefficient is measured directly as D_0.

The self-diffusion coefficient of the protein–detergent complex was measured using either the natural fluorescence of Bchl at 850 nm or the FLUOS fluorescence when the protein was labeled (with excitation at 488 nm). In both cases, the diffusion coefficient was found equal to $7 \pm 0.4\ 10^{-7}$ $cm^2\ s^{-1}$ (Table 2), which gives an hydrodynamic radius of 30 ± 2 Å. Because the radius of the bare OG micelles has been measured equal to 23.5 Å (Kameyama and Takagi, 1990), the higher value found here for R confirms that we measure the equivalent radius of the protein surrounded by a belt of OG. Indeed, according to crystallographic data for LH2 oligomers (MacDermott et al., 1995; Koepke et al., 1996; Ranck et al., 2001), the shape of the protein assembly can be described as a hollow cylinder where the external radius of the ring-like assembly is ~40 Å, and the transmembrane height is ~50 Å. We have then crudely modeled the LH2-OG complex by a solid ellipsoid of 25-Å-long minor semiaxis, a, and of major semiaxis b. Then, the Perrin's formulas (Berne and Pecora, 1976) have been used to determine b. The self-diffusion coefficient can be written as

$$D_0 = k_B T G(\rho)/6\pi\eta a \quad \text{where} \quad \rho = b/a$$

and

$$G(\rho) = \rho(\rho^2 - 1)^{1/2}\arctan[(\rho^2 - 1)^{1/2}] \quad \text{if} \quad \rho > 1 \quad \text{(oblate ellipsoid)},$$

or

$$G(\rho) = (1 - \rho^2)^{-1/2}\ln[(1 + (1 - \rho^2)^{1/2})/\rho] \quad \text{if} \quad \rho < 1 \quad \text{(prolate ellipsoid)}.$$

Taking $a = 25$ Å and $D = 7 \pm 0.4\ 10^{-7}$ $cm^2\ s^{-1}$, one founds $G(\rho) = 0.816 \pm 0.047$. $G(\rho) < 1$ corresponds to an oblate ellipsoid, and one finally founds $b = 33 \pm 1$ Å. The LH2-OG complex can thus be considered as a 50-Å-long and 66-Å large oblate ellipsoid. One may note that, in the micellar solution of another detergent, lauryl di-methyl-amine oxide, a diffusion coefficient D_0 equal to $2.5\ 10^{-7}$ $cm^2\ s^{-1}$ was measured by sedimentation velocity (Jirsakova et al., 1996a) (Table 2). Using the same procedure for this diffusion coefficient leads to an oblate ellipsoid of semiaxes $a = 25$ Å and $b = 27$ Å, values that are still in the same range. A difference in hydration of the surfactant polar heads, or in the protrusion of hydrophobic tails in the complex can explain the slight difference observed. These dimensions are yet in a range expected if one considers the crystallographic models of LH2 oligomers (MacDermott et al., 1995; Koepke et al., 1996; Ranck et al., 2001). The smaller values in micellar solution could indicate a more compact three-dimensional structure of the LH2 complex.

In the MO cubic phase, a control experiment was first performed by dissolving an amphiphilic probe, C_{18}FLUO, in the lipids. This probe is confined to the lipid bilayers with its alkyl chains in the hydrophobic core and the FLUO group at the lipid/water interface, as proved previously (Maldonado et al., 1997). Its self-diffusion coefficient in the cubic phase was found equal to $6.2 \pm 0.2\ 10^{-8}$ $cm^2\ s^{-1}$ at 22°C, in excellent agreement with previous measurements made in the same Q230 cubic phase, but using another C_{18} probe labeled at a carbon atom of the alkyl chain (Cribier et al., 1993) (Table 2). Because the self-diffusion coefficient is very sensitive with temperature (Eriksson and Lindblöm, 1993; Cribier et al., 1993), the value we have found is in rather good agreement with the self-diffusion coefficient determined by the pulse field gradient nuclear magnetic resonance method by Eriksson and Lindblom (1993) in a cubic phase of slightly different composition and at a different temperature.

Diffusion measurements were then achieved in the protein-containing cubic phase to check the LH2 complex incorporation. The Bchl infrared fluorescence could not be used for these measurements because it is quenched in this phase (see below), and we resorted to the FLUOS-labeled protein. The FLUOS-labeled LH2 self-diffusion coefficient measured in the lipidic cubic matrix is $1.4 \pm 0.2\ 10^{-8}$ $cm^2\ s^{-1}$ (Fig. 3 and Table 2). This value does not correspond to the self-diffusion coefficient in the bilayer itself. Anderson and Wennerström (1990) have shown that one

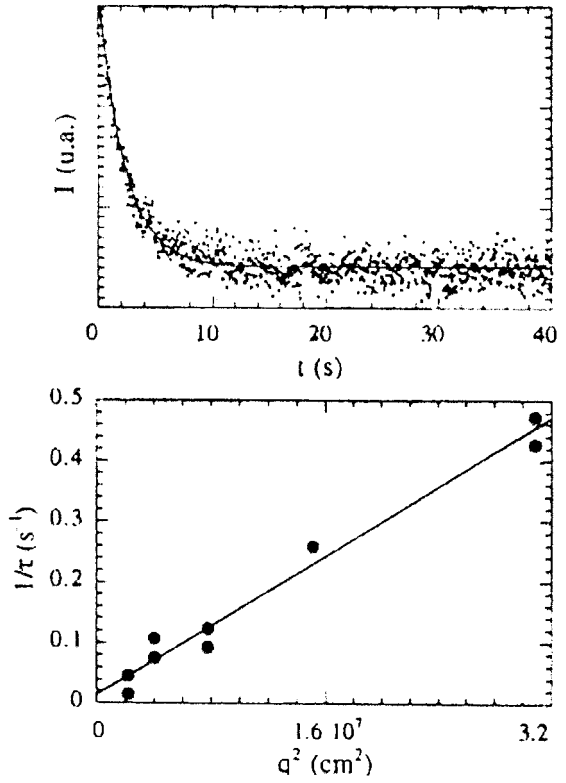

FIGURE 3 Decrease of the fringes contrast as a function of time for a LH2-containing cubic sample (characteristic time $\tau = 2.3 \pm 0.05$ s) (*top*). Variation of the reverse of the characteristic time as a function of the square wave vector q^2 (*bottom*). The slope of the best linear fit (*solid trace*) gives the self-diffusion coefficient of the protein in the cubic phase: here $1.4 \pm 0.2\ 10^{-8}$ cm^2 s^{-1}.

must take into account an obstruction factor due to the bilayer folding in three dimensions. The self-diffusion coefficient of a particle moving on the surface of the cubic phase is

$$D_s = D_{s0}(a_s + b_s\phi^2),$$

where ϕ is the volume fraction of polar components, a_s and b_s are numerical factors, and D_{s0} is the self-diffusion coefficient of the particle on a flat surface. $(a_s + b_s\phi^2)$ is the obstruction factor. $a_s = ⅔$ independently of the type of the cubic phase, whereas b_s depends on the minimal surface topology. Values of b_s have been calculated for the Schwartz primitive surface ($b_s = 0.45$), and for the I-WP surface ($b_s = 0.6$), but not for the *G* surface corresponding to the Q230 cubic phase. However, the structure of the *G* surface (Ia3d) is very close to that of the P and I-WP surfaces (Im3m) because it can be generated by a simple transformation of the P surface (Hyde et al., 1997). Thus, we have considered that the obstruction factor of the Q230 cubic phase could be calculated using Anderson and Wennerström (1990) theoretical framework for the P and I-WP surfaces, taking $\phi = \phi_{water} = 0.3$ in first approximation.

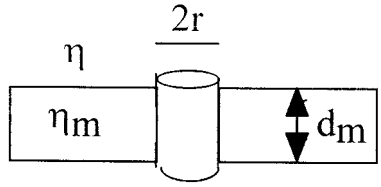

FIGURE 4 Schematic representation of the Saffman and Delbrück model: a cylinder of radius r is diffusing in a flat layer of viscosity η_m and thickness d_m, whereas the surrounding solvent has a viscosity η.

From the experimental determination of D_s, D_{s0} of the LH2 has been deduced. Both topologies lead to similar values: $D_{s0\text{-Fluos}} = 2.3 \pm 0.3\ 10^{-8}$ cm^2 s^{-1}. At this stage, we have used the Saffman and Delbrück (1975) model to relate the self-diffusion coefficient on the flat surface with the number of LH2 units composing the complex. These authors predict that the self-diffusion coefficient D_{s0} of a cylinder of radius r and height d_m diffusing in a flat sheet of viscosity η_m (Fig. 4) can be written as

$$D = \frac{k_B T}{4\pi\eta_m d_m}\left(\ln\frac{\eta_m d_m}{\eta r} - \gamma'\right),$$

where k_B is the Boltzmann constant, T is the temperature, η is the viscosity of the bounding fluid on both sides of the sheet, and γ' is Euler's constant (0.5772). d_m is also the thickness of the sheet (Fig. 4). The bilayer thickness is 35 Å (Briggs et al., 1996), so the only unknown parameter for the calculation of r is the viscosity of the bilayer.

To determine the bilayer viscosity, we have measured the self-diffusion coefficient of a fluorescent transmembrane peptide organized in an α-helix, whose radius is 5 Å (Setlow and Pollard, 1962): $D_{pep} = 2.4 \pm 0.2\ 10^{-8}$ cm^2 s^{-1} (Table 2). Using Anderson and Wennerström's (1990) theoretical framework to calculate the obstruction factor and Saffman and Delbrück's (1975) model, the MO bilayer viscosity η_m is found equal to 1.5 ± 0.15 P, in fair agreement with the values found in the literature (Fragata et al., 1984). This value was injected in Saffman and Delbrück expression to determine the radius of the diffusing LH2 complex in the cubic phase. It leads to a radius $r_{LH2} = 70 \pm 20$ Å. This result indicates that the protein is still oligomeric in the cubic phase. However, the value of r_{LH2} is almost twice larger than the radius measured for the nonameric ring by electron microscopy of LH2 two-dimensional crystals (Ranck et al., 2001). Fusion of nonamers into aggregates of a larger size could also be considered. Such aggregates should be, however, rather monodisperse, as indicated by the FRAP experiments (see Fig. 3). The presence of several lipids carried by the LH2 as it diffuses might also contribute to slow down the diffusion and might explain the radius determined experimentally. In contrast, the discrepancy could come from the harsh approximation of the protein as a solid cylinder. Thus, the size given for the diffusing

complex should be considered as a rough estimation, indicating mainly that the LH2 oligomers have not been disintegrated to smaller units (monomers, dimers, etc.) in the MO cubic phase.

The spectral properties of the LH2 complex are modified in the Q230 cubic phase

Figure 1 compares the absorption spectrum of the LH2 measured after its incorporation in the cubic phase to that of the protein in OG solution. Several modifications are obvious in the cubic phase: disappearance of the B800 Q_y band, appearance of a weak and broad band located at 770 nm, large blue-shift (about 20 nm) of the carotenoids absorption bands, and slight red-shift of the B850 Q_y band from 854 to 859 nm. These changes could be observed as soon as the cubic phase was formed, and did not evolve within one day. They were also observed when FLUOS-labeled LH2 was incorporated in the cubic phase.

Some of these changes have already been observed for LH2 from other purple bacteria in detergent solutions and attributed to the selective unbinding of the B800 Bchl molecules. Earlier experiments indicated that B800 Bchls are rather easily removed from their binding site, giving rise to the disappearance of the 800-nm band and formation of a 770–790-nm band attributed to free Bchl. Similar observations were done for *Rv. gelatinosus* LH2 in presence of a mild ionic detergent, lithium dodecyl sulfate (Jirsakova, 1995). More recently, the B800 Bchl removal was shown to be reversible, the empty binding sites being able to again incorporate Bchl molecules or even some Bchl derivatives (Bandilla et al., 1998; Fraser et al., 1999; Gall et al., 1999). It was also shown that the B800 removal occurred without perturbing deeply the structure of the LH2 complex. The B850 assembly and that of the carotenoid did not change as deduced from the absorption and dichroism spectra (Fraser et al., 1999), and the interactions of B850 with the protein scaffold were not modified (Gall et al., 1999).

In line with these studies, the suppression of the 800-nm absorption band and the formation of the weak 760-nm one indicated that the B800 Bchl molecules were released from their binding sites when LH2 was incorporated in the cubic phase. But here, the carotenoid binding site(s) was altered at the same time. Yet the B850-Bchl molecules, which are central to the LH2 structure, were only slightly affected. Their red shift could be attributed to their new lipid environment; indeed in the membrane-bound state, *Rv. gelatinosus* LH2 maximally absorbs at 857 nm. Thus the structure of the LH2 in the cubic phase was presumably modified, mostly by displacement of the B800 Bchl molecules and by modifications of the carotenoid environment (or conformation), but the overall structure was probably not fully disrupted.

These structural rearrangements were accompanied with Bchl fluorescence changes. Figure 2 *A* shows the fluorescence emission of an LH2 sample in OG solution, when excited at 488 nm: the emission mainly comes from the B850-Bchls, with a minor component originating from uncoupled B800-Bchls. In contrast, the emission band at 850 nm was suppressed when a LH2 sample was incorporated in the cubic phase (Fig. 2 *B*). Only a strong and wide band at ~660 nm was observed, presumably due to damaged pigments. The same observations were done for FLUOS-labeled LH2 (not shown). We measured also the fluorescence emission of LH2 in a solution containing mixed OG/MO micelles (Fig. 2 *B*). In this case, an emission band at 850 nm originating from B850-Bchl was observed, as well as the 660-nm emission band. This fluorescence spectrum was stable for weeks. The fluorescence quenching observed in the cubic phase was thus not due to monoolein by itself. It might occur because the transfer of excitation between carotenoids and B850-Bchl was inefficient, as a result of the modifications also detected by absorbance measurements.

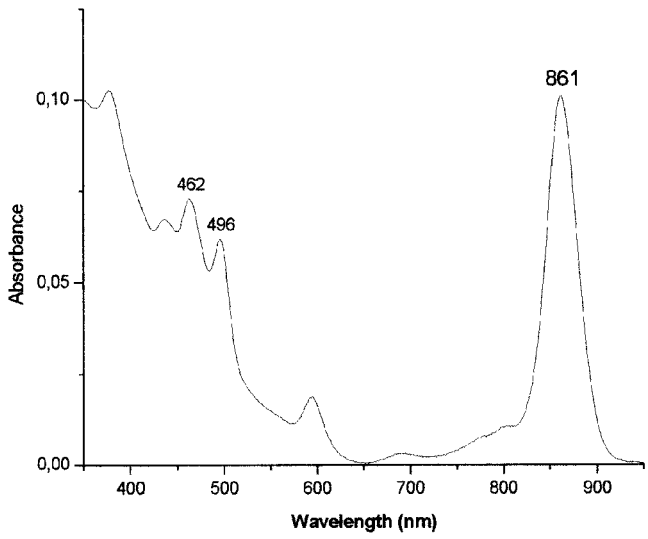

FIGURE 5 Absorption spectrum of a LH2 sample after its incorporation in the MO L_α phase at 25°C. The aqueous solution is a 50 mM BisTris-propane buffer, pH 9.0, containing 0.1 M NaCl and 27 mM OG.

To check whether the curvature of the cubic phase could be responsible of the spectroscopic modifications, the LH2 was incorporated in a lamellar phase of MO. The absorption spectrum of the protein in the lamellar phase is quite similar to what has been observed in the cubic phase (Fig. 5). This result proves that the spectral modifications originate from the high MO concentration (and low water content) and not from the strain exerted by the bilayer curvature on the protein.

CONCLUSION

In this work, the LH2 complex was incorporated into the Q230 cubic phase of MO by mixing a micellar OG solution of the protein with the monoglyceride at a defined water

content. Control experiments were also performed with OG alone, in the absence of protein, to verify that, under our experimental conditions, the detergent did not modify the cubic phase in the range of concentrations corresponding to our protocols. Low protein concentrations (corresponding to 1 $\alpha\beta$ subunit per ~50,000 MO molecules) did not perturb the structure of the cubic phase, as shown by small-angle scattering and by the isotropy of the mixture, and the protein was evenly distributed in the phase, which was homogeneous in color. The LH2 hydrophobic transmembrane domain was presumably localized within the lipid bilayers in contact with the MO hydrocarbon chains, with its hydrophilic surfaces anchored at the polar/apolar surfaces of the water channels. At a higher protein concentration (~1 $\alpha\beta$ subunit per 5000 MO molecules), the phase diagram changed and a transition to the lamellar L_α phase occurred. A similar polymorphism has been observed for bacteriorhodopsin/MO system (W. Rowe, University of Manchester Institute of Science and Technology, Manchester, U.K., personal communication).

We used FRAP measurements to determine whether these modifications alter the oligomeric structure of the protein in the cubic phase. The self-diffusion coefficient of LH2 is a significant parameter that corresponds to the size of the diffusing oligomer. We have used the Saffman and Delbrück (1975) model, and taken into account the obstruction factor modeled by Anderson and Wennerström (1990), to determine the radius of the protein diffusing in the cubic phase, with a simple cylindrical model. We have found a radius of 70 Å, i.e., bigger than the dimension determined by electron microscopy in planar lipid bilayers (Ranck et al., 2001). From this comparison, we can conclude that the LH2 is still oligomeric in the cubic phase, in agreement with the maintenance of the B850 Bchls binding site. With this cylindrical model, the lateral dimensions of the LH2 aggregates (in the bilayer plane) would be similar to the unit cell parameter of the cubic phase. The plasticity of the bilayers, however, might permit accommodation of such large protein domains, especially when the protein is incorporated in very low amount as in our experiments (see above). In connection with this, one may remark that a large membrane protein such as *Rhodopseudomonas* (*Rps*.) *viridis* reaction center was incorporated in the cubic phase (Chiu et al., 2000) despite the fact that one of its overall dimensions measures 130 Å, and that the size of its hydrophilic domains exceeds that of the aqueous channels. Moreover, we stress that the approximations done in the interpretation of the diffusion coefficient are crude (see Discussion). The dimensions found for the model are compatible with the presence of oligomers, but they should not be taken at their face value and do not allow precise estimation of the number of subunits.

Several spectroscopic methods were used to characterize the state of the protein at high dilution in the cubic phase. For these experiments, we used either the native protein or the protein modified by coupling with a fluorescent label. The label did not modify the spectral properties of the bound pigments and was probably reacting with residues exposed at the hydrophilic surfaces.

Inclusion in the cubic phase induced several modifications of the chromophores. The loss of the B800-Bchl was indicative of a disorganization of the binding site of this pigment and of the breakage of its interactions with the protein (such as ligand- and H-bonds, and Van der Waals contacts). In the LH2 structures presently known at atomic resolution, this Bchl is less buried than the B850 ones. It is liganded to a residue of the α N-terminal chain and partly accessible to the external surface of the protein (MacDermott et al., 1995; Koepke et al., 1996). After its removal from *Rps. acidophila* LH2, B800 could be reversibly rebound in vitro (Fraser et al., 1999). The absence of B800 in the cubic phase could therefore have reflected a minor structural change, limited to this binding site and without influence on the overall structure of the oligomer. However, two other concomitant changes were indicative of a more profound disorder: the large blue shift of the carotenoids, and the loss of the B850-Bchl fluorescence. The absorption properties of carotenoids are modulated by the polarizability of the surrounding medium. In the two crystallographic LH2 structures, the carotenoid molecule is extended in an all-*trans* conformation from the cytoplasmic to the periplasmic surfaces. It is in van der Waals contacts with several residues and in extensive ones with the phytyl tails of the Bchls. These contacts contribute to the stability of the oligomeric assembly. The blue shift of the carotenoids absorption in the cubic phase, as compared to LH2 in vivo and in detergent solution, indicates a new environment of their conjugated double-bound system, which is located in the hydrophobic core of the protein. The quenching of B850 fluorescence probably results of the same structural changes, which could alter the energy transfer between chromophores. Altogether, these spectral shifts indicate a weakening of the pigment–pigment and pigment–protein interactions, affecting not only the B800 binding site but also the hydrophobic core of the LH2 structure.

We tried to determine the physical parameters responsible for the observed spectroscopic changes. Because the spectral properties of the protein are modified in both the lamellar and in the Q230 phases of MO, the strain exerted on the oligomeric protein by the curvature of the bilayers in the cubic phase does not play a role. The spectroscopic modifications may originate from the high MO content (or low water content) because the Bchl fluorescence was not quenched in the presence of MO in mixed OG/MO solutions. It should be noted that this is the first case where structural modifications are reported for a membrane protein after its inclusion in the Q230 cubic phase of MO. In contrast, bacteriorhodopsin kept its native structure, and could be crystallized with a full occupancy of the retinal chromophore (Heberle et al., 1998). Bacteriorhodopsin is

known to be extremely stable. Furthermore, it was shown to cocrystallize with its own lipids which excluded direct contacts with MO (Luecke et al., 1999; Nollert et al., 1999). Recently, halorhodopsin and two bacterial reaction centers were successfully crystallized in the cubic phase, as judged by their x-ray diffraction patterns (Chiu et al., 2000). In the same work, microcrystals of *Rps. acidophila* LH2 were also grown from the cubic phase, but their quality was not sufficient for an x-ray study. It would be interesting to determine the spectroscopic properties of these LH2 crystals. A comparison with our results would indicate whether the poor stability in the cubic phase of *Rv. gelatinosus* LH2 is an exceptional case, or whether it is shared by other membrane proteins of the same structural family.

Despite our observations, is it worth undertaking crystallization of this protein from the cubic phase? The cubic phase mainly provides a matrix and the crystal growth occurs out of the phase (Caffrey, 2000). One could argue that, even if the protein had adopted an intermediate structure within the cubic phase, it could come back to its native state during its crystallization. From this point of view, this LH2 would be a good test for this hypothesis. However, this crystallization would be challenging, because renaturation of the protein would require putting back all the lost B800 chromophores in their binding site, probably at the expense of added free Bchl. Incomplete binding would result in protein microheterogeneities, a feature known to interfere with crystal growth (Lorber and Giegé, 1999).

Other bicontinuous mesophases should also be considered as potential matrices for transmembrane protein crystallization, such as the sponge-like phases (Strey et al., 1990). The sponge-like phase consists of an unordered multiconnected bilayer of surfactant (possibly with cosurfactant) separating water into two distinct spaces. This isotropic phase is highly hydrated and not as viscous as the cubic phase and thus easier to handle. However, the high concentration of surfactant or cosurfactant might be a factor of protein denaturation.

The authors would like to thank Martin Caffrey for his advice, M. Waks for careful reading, José Quintas for his help in building the mixing device, and Mrs M.C. Gonnet for her help in biochemical preparations. We are grateful to Mark Chiu and William Rowe for sharing results before publication, and to Bernadette Arnoux, Stephen Hyde, Sophie Cribier, and the reviewers for helpful comments.

This work was supported in part by a grant from the Centre National de la Recherche Scientifique (Programme Physique et Chimie du Vivant). N.T. acknowledges partial financial support from the Société de Secours des Amis des Sciences.

REFERENCES

Ai, X., and M. Caffrey. 2000. Membrane protein crystallization in lipidic mesophases: detergent effects. *Biophys. J.* 79:394–405.

Anderson, D. M., and H. Wennerström. 1990. Diffusion in bicontinuous cubic phases, L3 phase and microemulsions. *J. Phys. Chem.* 94: 8683–8694.

Bandilla, M., B. Ucker, M. Ram, I. Simonin, E. Gelhaye, G. McDermott, R. J. Cogdell, and H. Scheer. 1998. Reconstitution of the B800 bacteriochlorophylls in the peripheral light harvesting complex B800–850 of Rhodobacter sphaeroides 2.4.1 with BChl a and modified (bacterio) chlorophylls. *Biochim. Biophys. Acta.* 1364:390–402.

Berne, B. J., and R. Pecora. 1976. Dynamic Light Scattering with Applications to Chemistry, Biology and Physics. John Wiley and Sons, Inc., New York.

Briggs, J., H. Chung, and M. Caffrey. 1996. The temperature-composition phase diagram and mesophase structure characterization of the monoolein/water system. *J. Phys. II France.* 6:723–751.

Brunisholz, R. A., F. Suter, and H. Zuber. 1994. Structural and spectral characterization of the antenna complexes of *Rhodocyclus gelatinosus*. Indications of a hairpin-like-arranged antenna apoprotein with an unusually high alanine content. *Eur. J. Biochem.* 222:667–675.

Caffrey, M. 1987. Kinetics and mechanism of transitions involving the lamellar, cubic, inverted hexagonal, and fluid isotropic phases of hydrated monoacylglycerides monitored by time-resolved X-ray diffraction. *Biochemistry.* 26:6349–6363.

Caffrey, M. 2000. A lipid's eye view of membrane protein crystallization in mesophases. *Curr. Opin. Struct. Biol.* 10:486–497.

Cheng, A., B. Hummel, H. Qiu, and M. Caffrey. 1998. A simple mechanical mixer for small viscous lipid-containing samples. *Chem. Phys. Lipids.* 95:11–21.

Chiu, M. L., P. Nollert, M. C. Loewen, H. Belrhali, E. PebayPeroula, J. P. Rosenbusch, and E. M. Landau. 2000. Crystallization in cubo: general applicability to membrane proteins. *Acta Cryst. D.* 56:781–784.

Cribier, S., A. Gulik, P. Fellman, R. Vargas, P. F. Devaux, and V. Luzzati. 1993. Cubic phases of lipid-containing systems. A translational diffusion study by fluorescence recovery after photobleaching. *J. Mol. Biol.* 229: 517–525.

Eriksson, P. O., and G. Lindblöm. 1993. Lipid and water diffusion in bicontinuous phases measured by NMR. *Biophys. J.* 64:129–136.

Evans, G. T., and C. P. James. 1983. Self-diffusion coefficient for Brownian particles. *J. Chem. Phys.* 79:5553–5557.

Fragata, M., S. Ohnishi, K. Asada, T. Ito, and M. Takahashi. 1984. Lateral diffusion of plastocyanin in multilamellar mixed-lipid bilayers studied by fluorescence recovery after photobleaching. *Biochemistry.* 23: 4044–4051.

Fraser, N. J., P. J. Dominy, B. Ucker, I. Simonin, H. Scheer, and R. J. Cogdell. 1999. Selective release, removal, and reconstitution of bacteriochlorophyll a molecules into the B800 sites of LH2 complexes from *Rhodopseudomonas acidophila* 10050. *Biochemistry.* 38:9684–9692.

Freer, A., S. Prince, K. Sauer, M. Papiz, A. Hawthornwaite-Lawless, G. McDermott, R. Cogdell, and N. W. Isaacs. 1996. Pigment–pigment interactions and energy transfer in the antenna complex of the photosynthetic bacterium *Rhodopseudomonas acidophila*. *Structure.* 4:449–462.

Gall, A., N. J. Fraser, M. C. Bellisent-Funel, H. Scheer, B. Robert, and R. J. Cogdell. 1999. Bacteriochlorin–protein interactions in native B800–B850, B800 deficient and B800-Bchla$_p$-reconstituted complexes from *Rhodopseudomonas acidophila*, strain 10050. *FEBS Lett.* 449: 269–272.

Guinier, A. 1952. X-ray Crystallographic Technology. Hilger and Watts Ltd, London.

Heberle, J., G. Buldt, E. Koglin, J. P. Rosenbusch, and E. M. Landau. 1998. Assessing the functionality of a membrane protein in a three-dimensional crystal. *J. Mol. Biol.* 281:587–592.

Hyde, S., K. Anderson, Z. Blum, T. Landh, S. Lidin, and B. W. Ninham. 1997. The Language of Shape. Elsevier, Amsterdam.

Jirsakova, V. 1995. Caractérisation structurale et fonctionnelle des antennes collectrices de lumière de la bactérie pourpre *Rubrivivax gelatinosus*. Doctoral dissertation, Université de Paris-Sud, Orsay, France.

Jirsakova, V., F. Reiss-Husson, and J. L. Ranck. 1996a. Oligomeric state of the light-harvesting complexes B800–850 and B875 from purple bacterium *Rubrivivax gelatinosus* in detergent solution. *Biochim. Biophys. Acta.* 1277:150–160.

Jirsakova, V., F. Reiss-Husson, B. Vandijk, G. Owen, and A. J. Hoff. 1996b. Characterization of carotenoid triplet states in the light-harvesting complex B800–850 from the purple bacterium *Rubrivivax gelatinosus*. *Photochem. Photobiol.* 64:363–368.

Kameyama, K., and T. Takagi. 1990. Micellar properties of octylglucoside in aqueous solutions. *J. Colloid Interf. Sci.* 137:1–10.

Koepke, J., X. Hu, C. Muenke, K. Schulten, and H. Michel. 1996. The crystal structure of the light-harvesting complex II (B800–850) from *Rhodospirillum molischianum*. *Structure.* 4:581–597.

Landau, E. M., and J. P. Rosenbusch. 1996. Lipidic cubic phases: a novel concept for the crystallization of membrane proteins. *Proc. Natl. Acad. Sci. U.S.A.* 93:14532–14535.

Landau, E. M., G. Rummel, S. W. Cowan-Jacob, and J. P. Rosenbusch. 1997. Crystallization of a polar protein and small molecules from the aqueous compartment of lipidic cubic phases. *J. Phys. Chem. B.* 101: 1935–1937.

Larsson, K. 1983. Two cubic phases in monoolein–water system. *Nature.* 304:664.

Lorber, B., and R. Giegé. 1999. Biochemical aspects and handling of macromolecular solutions and crystals. *In* Crystallization of Nucleic Acids and Proteins, A Practical Approach. A. Ducruix and R. Giegé, editors. Oxford University Press, Oxford, UK. 17–43.

Luecke, H., B. Schobert, H. T. Richter, J. P. Cartailler, and J. K. Lanyi. 1999. Structure of bacteriorhodopsin at 1.55 angstrom resolution. *J. Mol. Biol.* 291:899–911.

Luzzati, V., H. Delacroix, A. Gulik, T. Gulik-Krzywicki, P. Mariani, and R. Vargas. 1997. The cubic phases of lipids. *Curr. Top. Membr.* 44: 3–24.

MacDermott, G., S. M. Prince, A. A. Freer, A. M. Hawthornethwaite-Lawless, M. Z. Papiz, R. J. Cogdell, and N. W. Isaacs. 1995. Crystal structure of an integral membrane light-harvesting complex from photosynthetic bacteria. *Nature.* 374:517–521.

Maldonado, A., W. Urbach, and D. Langevin. 1997. Surface self-diffusion in L3 Phases. *J. Phys. Chem. B.* 101:8069–8073.

Messager, R., A. Ott, D. Chatenay, W. Urbach, and D. Langevin. 1988. Are giant micelles living polymers? *Phys. Rev. Lett.* 60:1410–1413.

Nollert, P., A. Royant, E. PebayPeyroula, and E. M. Landau. 1999. Detergent-free membrane protein crystallization. *FEBS Lett.* 457:205–208.

Qiu, H., and M. Caffrey. 2000. The phase diagram of the monoolein/water system: metastability and equilibrium aspects. *Biomaterials.* 21: 223–234.

Ranck, J. L., T. Ruiz, G. Péhau-Renaudet, B. Arnoux, and F. Reiss-Husson. 2001. Two-dimensional structure of the native light-harvesting complex LH2 from *Rubrivivax gelatinosus* and of a truncated form. *Biochim. Biophys. Acta.*, 1506:67–68.

Rummel, G., A. Hardmeyer, C. Widmer, M. L. Chiu, P. Nollert, K. P. Locher, I. Pedruzzi, E. M. Landau, and J. P. Rosenbusch. 1998. Lipidic cubic phases: new matrices for the three-dimensional crystallization of membrane proteins. *J. Struct. Biol.* 121:82–91.

Saffman, P. G., and M. Delbrück. 1975. Brownian motion in biological membranes. *Proc. Natl. Acad. Sci. U.S.A.* 72:3111–3113.

Savage, H., M. Cyrclaff, G. Montoya, W. Kühlbrandt, and I. Sinning. 1996. Two-dimensional structure of light harvesting complex (LHII) from the purple bacterium *Rhodovulum sulfidophilum* and comparison with LHII from *Rhodopseudomonas acidophila*. *Structure.* 4:243–252.

Schägger, H., and G. VonJagow. 1987. Tricine-sodium dodecyl sulfate-polyacrylamide gel electrophoresis for the separation of proteins in the range from 1 to 100 kDa. *Anal. Biochem.* 166:368–379.

Sereda, T. J., C. T. Mant, A. M. Quinn, and R. S. Hodges. 1993. Effect of the alpha-amino group on peptide retention behavior in reversed-phase chromatography. Determination of the pKa values of the alpha-amino group of nineteen different N-terminal aminoacid residues. *J. Chromatogr.* 646:17–30.

Setlow, R. B., and E. C. Pollard. 1962. Molecular Biophysics. Adison Wesley, London.

Strey, R., W. Jahn, G. Porte, and P. Bassereau. 1990. Freeze fracture electron microscopy of dilute lamellar phase and anomalous isotropic (L3) phases. *Langmuir.* 6:1635–1639.

Walz, T., and R. Ghosh. 1997. Two-dimensional crystallization of the light-harvesting I - Reaction centre photounit from *Rhodospirillum rubrum*. *J. Mol. Biol.* 265:107–111.